Research Article | Vol. 27, No. 5 | 4 Mar 2019 | OPTICS EXPRESS 6106
Optics EXPRESS

Frequency metrology of molecules in the near-infrared by NICE-OHMS

T.-P. Hua[1], Y.R. Sun[1,2,*], J. Wang[1], A.-W. Liu[1,2], S.-M. Hu[1,2]

[1] *Hefei National Laboratory for Physical Sciences at Microscale, iChem center, University of Science and Technology of China, Hefei 230026, China*
[2] *CAS Center for Excellence in Quantum Information and Quantum Physics, University of Science and Technology of China, Hefei 230026, China*
* *robert@ustc.edu.cn*

Abstract: Noise-immune cavity enhanced optical heterodyne molecular spectroscopy (NICE-OHMS) is extremely sensitive in detecting weak absorption. However, the use of NICE-OHMS for metrology study was also hindered by its sensitivity to influence from various experimental conditions such as the residual amplitude modulation. Here we demonstrate to use NICE-OHMS for precision measurements of Lamb-dip spectra of molecules. After a dedicated investigation of the systematic uncertainties in the NICE-OHMS measurement, the transition frequency of a ro-vibrational line of C_2H_2 near 789 nm was determined to be 379 639 280 915.3±1.2 kHz (fractional uncertainty 3.2×10^{-12}), agreeing well with, but more accurate than, the value determined from previous cavity ring-down spectroscopy measurements. The study indicates the possibility to implement the very sensitive NICE-OHMS method for frequency metrology of molecules, or a molecular clock, in the near-infrared.

1. Introduction

Precise frequency measurements of molecular transitions play an essential role in widespread applications, such as frequency metrology [1], astronomy [2,3], and molecular spectroscopy [4,5]. There are also increasing interests to use precise molecular transitions to test the quantum electrodynamics (QED) theory [6–8], to determine fundamental physical constant [9] or to verify its stability [10–13], and to search parity-violating effects in chiral molecules [14, 15]. Moreover, reliable molecular frequencies are also candidates for optical clocks [16].

However, molecular lines in the near-infrared are mostly overtone transitions, which are orders of magnitude weaker than fundamental transitions [17, 18]. Precision spectroscopy of those lines requires highly sensitive detection methods. The sensitivity of detection can be considerably improved by using cavity enhancement absorption spectroscopy (CEAS) [19, 20], which takes advantage of a high finesses optical cavity to increase the optical path length. Since CEAS directly detects the change of transmitted laser power, the sensitivity is limited by the fluctuation of probe laser power and the $1/f$ noise. Cavity ring-down spectroscopy (CRDS) [21,22] measures the exponential decay of the laser power inside the resonant cavity, which is naturally immune to the laser power noise, leading to considerable improvement on the sensitivity [23]. The noise immune cavity enhanced optical heterodyne molecular spectroscopy (NICE-OHMS) technique combines the advantage of frequency modulation for reduction of noise and that of the cavity enhancement of the absorption path. The modulation frequency used in NICE-OHMS is set equal to the cavity free spectral range, which also considerably reduces the laser frequency noise. The technique was demonstrated as a frequency reference at 1064 nm by Ye et al. [24, 25]. Since then, this extremely sensitive technique, was applied in the studies of precision measurements of molecules [26, 27] and trace gas analysis [28, 29]. Recently, Zhao et.al. [30] reported a new result of noise equivalent absorption per unit length (NEAL) of 2.3×10^{-13} $cm^{-1}Hz^{-1/2}$, being close to the shot noise limit.

#352888 https://doi.org/10.1364/OE.27.006106
Journal © 2019 Received 27 Nov 2018; revised 18 Jan 2019; accepted 22 Jan 2019; published 20 Feb 2019

Optics EXPRESS

The high-finesse optical resonant cavity not only enhances the effective absorption path length, but also significantly enhances the light power in the cavity. Therefore, it allows saturation spectroscopy using low-power continuous-wave lasers [31]. Recently we have realized Lamb-dip measurements of ro-vibrational transitions of $^{12}C^{16}O$ at 1.57 μm with an uncertainty of 0.5 kHz [32] using comb-locked CRDS [32, 33]. In general, the NICE-OHMS technique is more sensitive than CEAS and CRDS, but as far as we know, there is no metrology study using NICE-OHMS toward an accuracy around 1 kHz in the near-IR region. In this paper, we report a comparison between NICE-OHMS and CRDS in metrology study of molecules, by measuring the Doppler-free saturated absorption spectrum of an acetylene line near 789 nm which has been recently measured by CRDS [34]. As will be shown in the following sections, the NICE-OHMS technique, being more sensitive than the relatively simple CRDS technique, needs dedicated investigations of various experimental conditions to eliminate systematic uncertainties, before it could be used as a technique for frequency metrology of molecules. We demonstrated to use NICE-OHMS to precisely determine the center of the acetylene line, agreeing well with that we obtained from CRDS. Moreover, we implemented an optical reference with a stability of 3×10^{-13} by locking a laser at the molecular line center using NICE-OHMS.

2. Experimental

The configuration of the experimental setup is shown in Fig 1. The 45.9-cm-long high-finesse (F = 67 000) cavity comprises a pair of high-reflective mirrors (Layertec, 1m radius of curvature), with one of the mirrors mounted on a piezoelectric actuator (PZT). The optical cavity is temperature stabilized at 25°C with a drift well below 10 mK/hour. The cavity is enclosed in a vacuum chamber which is also used as a heat reservoir. An external-cavity diode laser (Toptica DL100) with an output power of 40 mW, operating at around 778 nm, is locked to the optical cavity using the Pound-Drever-Hall (PDH) method [35]. Part of the laser beam is split for the frequency calibration, while the main beam first passes through an acousto-optics modulator (AOM), then is phase modulated by a fiber based electro-optic modulator (EOM Eospace PM-0K5-PFA-PFA-800UL). The EOM is temperature-stabilized by a TEC unit. Two frequencies, f_{PDH} about 20MHz and f_{FSR} about 327MHz, are simultaneously coupled into the EOM through a radio-frequency power combiner.

A small part of the beam was split from the main beam, and two detectors (PD1 and PD2) were used to monitor the laser power drift and the parasitic residual amplitude modulation (RAM) effects [36], respectively. A feedback circuits, the "power servo", was applied on the AOM to stabilize the laser power. Another feedback circuits, the "RAM servo", was also applied to reduce the RAM effect (will be discussed later). The beam reflected from the cavity is detected by a photo-receiver (PD3), and the signal is divided to lock the laser frequency to the cavity mode via the PDH scheme and to lock f_{FSR} to the cavity free spectral range frequency with the DeVoe-Brewer (DVB) scheme [37]. The beam transmitted through the cavity is collected with a high-speed photo-receiver (PD4) and then demodulated at the frequency f_{FSR} by a doubly balanced mixer (DBM). The resulted signal from the DBM is amplified to retrieve the dispersion signal of fm-NICE-OHMS. When a dither frequency of about 200 Hz was applied to the piezoelectric actuator attached on the HR mirror, $1f$ or $2f$ wavelength modulated (WM) NICE-OHMS signals can be obtained by a lock-in amplifier (SR830). The cavity length is stabilized through the piezoelectric actuator driven by a phase-lock circuit based on the beat signal between the laser and an optical frequency comb. The frequency comb is synthesized by an Er-fiber Oscillator operated at 1.56 μm. Its repetition frequency (f_R about 184MHz) and the carrier offset frequency (f_0) are both referenced to a GPS-referenced rubidium clock (GPS Reference-2000).

Optics EXPRESS

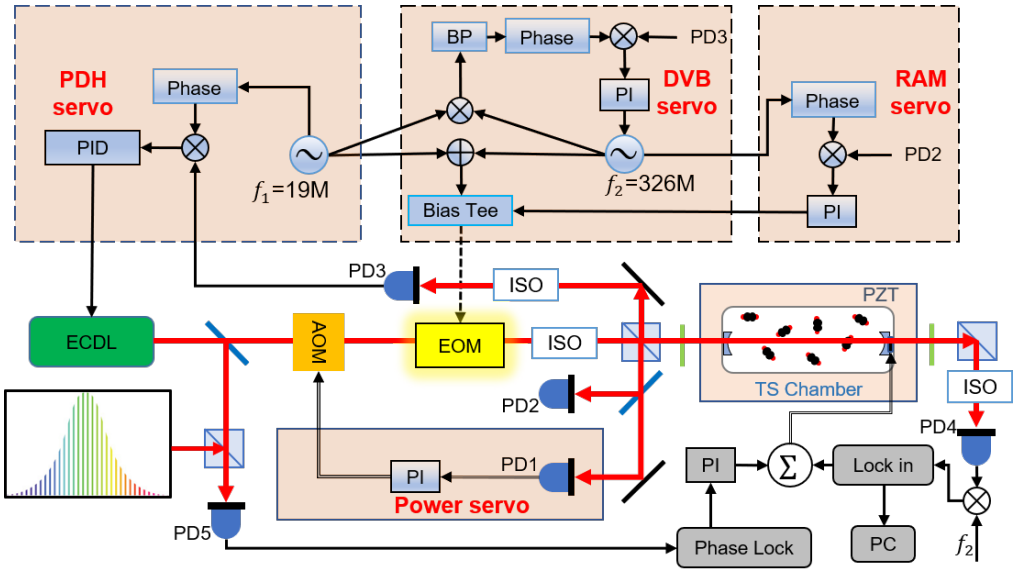

Fig. 1. Configuration of the NICE-OHMS experimental setup. An external-cavity diode laser (ECDL) is locked to the optical cavity using the PDH method, and sent through an EOM to impose both frequencies f_{PDH} and f_{FSR}. The laser power fluctuation is monitored by PD1 and controlled by the AOM modulator. Extra Residual amplitude modulation is recorded by PD2 and controlled by the RAM servo. The signal of the beam reflected from the cavity is recorded by a photo-diode PD3, used for both PDH servo and DVB servo. An addition cavity-length dither modulation with a frequency of f_{dith} is applied for lock-in detection. The beat signal between the probe laser and an optical frequency comb is used to lock the laser frequency through the feedback sent to the piezoelectric actuator attached on a cavity mirror.

3. Results and discussion

The C_2H_2 sample was purified by a liquid-N_2 ethanol solution trap before use. The P(5) line in the $\nu_1+3\nu_3$ band of C_2H_2 is located at 12663.403 cm^{-1}, with an intensity of 1.5×10^{-23} cm/molecule and an Einstein coefficient of 0.03 s^{-1} [38]. The transition dipole moment is 0.26mD. The saturation power is estimated to be about 38 kW cm^{-2}. In our measurements, the intra-cavity light power was about 13 W. Taking into account a laser beam waist radius of 0.5 mm, we estimate that the saturation parameter was about 0.1.

Fig. 2 shows the spectrum recoded at a pressure of 1.5 Pa. Both the dispersion signal of fm-NICE-OHMS and wm-NICE-OHMS signals were recorded. Each scan takes about 50 seconds, with a frequency step of 160 kHz and an averaging time about 1 s. For comparison, a CRDS spectrum is also given in Fig. 2. The CRDS scan took about 71 seconds. Because of the residual amplitude modulation and laser power fluctuation, there is a baseline drift in the dispersion signal of fm-NICE-OHMS, and the sensitivity is comparable to CRDS. The drift is considerably reduced in the $1f$ wm-NICE-OHMS signal, and the signal-to-noise ratio (SNR) is about 10 times of that in CRDS. In the $2f$ wm-NICE-OHMS spectrum, both the noise level and the signal amplitude decrease, result in a SNR similar to the $1f$ spectrum.

The NICE-OHMS line parameters such as the peak center and line-width are derived using the method similar to that given by Axner [28, 39]. The sub-Doppler $1f$ wm-NICE-OHMS spectra, detected at the first harmonic of the WM dither frequency, can be described as a product of a signal strength and the first Fourier coefficient of a Lorentzian dispersion function.

Optics EXPRESS

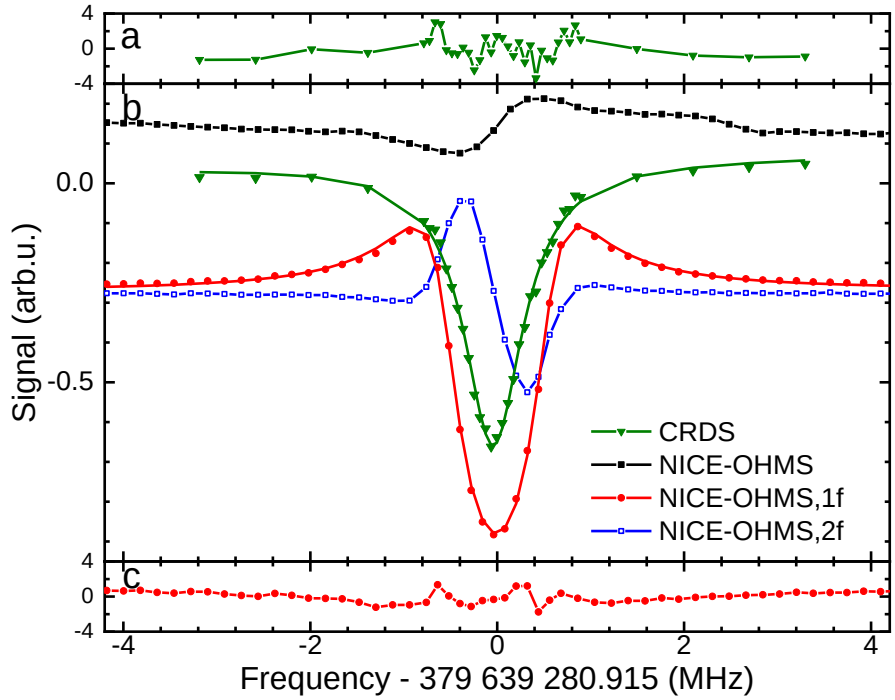

Fig. 2. Lamb-dip spectrum of P(5) line in the $\nu_1 + 3\nu_3$ band of $^{12}C_2H_2$ recorded by different methods (b). Acetylene sample pressure was 1.5 Pa. As for amplitude of the absorption signal, the Lamb dip obtained from CRDS has a depth of 4×10^{-9} cm^{-1}. Fitting residuals (all multiplied by a factor of 100) of the CRDS and $1f$ wm-NICE-OHMS spectra are shown in (a) and (c), respectively.

Compared to the CRDS method, more sophisticated frequency modulation and wavelength modulation are used in NICE-OHMS measurements. We found that the line center determined from the fit of the NICE-OHMS spectrum could be sensitive to some of the experimental conditions. In order to determine the line position precisely, we investigated various conditions which may raise systematic shift on the line center and these effects are described below.

WM-modulation amplitude and frequency - Wavelength modulation is made by dithering the cavity length through the piezo actuator. This modulation helps to eliminate the slow baseline drift in the dispersion NICE-OHMS signal which often comes from residual amplitude modulation (RAM) in the frequency modulation or other etalon effects [40]. However, special caution must be paid since the modulation could also impose distortions on the line profile. To properly assess the systematic effect due to the modulation, different modulation amplitudes and modulation frequencies were applied and the line centers were derived by fitting the spectra obtained at different conditions. The results are depicted in Fig. 3. The modulation amplitude was first fixed at about 0.6 MHz, and the modulation frequency varied between 100 Hz and 800 Hz. When a modulation frequency of over 300 Hz was applied, there would be a considerable shift on the line centers obtained from the fit of the spectrum. Meanwhile, choosing a very low modulation frequency will result in an increasing noise level. Similar effect appeared when we fixed the modulation frequency at 200 Hz and changed the modulation amplitude up to over 1 MHz. A possible reason is, due to the limited bandwidth and gain of the feedback

servo for locking the laser to the cavity, when the modulation amplitude or the modulation frequency is too large, the laser frequency cannot follow the change of the cavity mode frequency, which results in distortion of the line shape. Therefore, for precision spectroscopy towards sub kHz uncertainty, the modulation conditions must be carefully chosen. In our case, we chose a modulation frequency of 200 Hz and an amplitude of 0.3 MHz, confirming that the influence should be well below the statistical uncertainty.

Residual amplitude modulation - The fiber electro-optic modulator used for phase modulation could modulate the laser power as well, which is the so called residual amplitude modulation (RAM). RAM can rise from the Fabry-Pérot etalon effect due to reflections from facets of the EOM crystal and other reflective surfaces [36,41], from beam polarization effects [42], or from thermal effects in the EOM medium [36,41,42]. All these effects ultimately limit the sensitivity and the accuracy of the measurement. In order to suppress this effect, we used a method based on an active servo at the output of the EOM [36]. A radio-frequency (RF) spectrometer was used to monitor the signal recorded by PD2. We use the RF power at 327MHz divided by the total laser power as a measure of the RAM amplitude. A feedback servo was used to reduce the RAM signal. As shown in Fig. 3, when the RAM amplitude is below -20 dB, no detectable RAM-induced line shift was found in our WM-NICE-OHMS measurements.

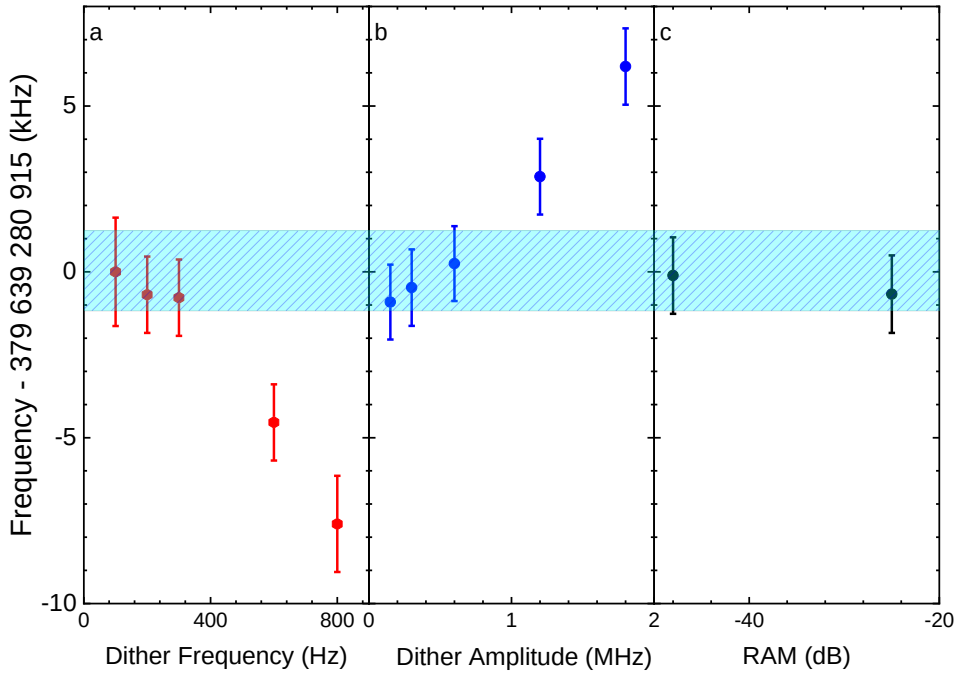

Fig. 3. Systematic shifts in the $1f$ wm-NICE-OHMS measurements. Influence of choosing different frequencies and amplitudes in the wavelength modulation are given in (a) and (b), respectively. The effect of the residual amplitude modulation (RAM) is shown in (c). The shaded region represents 1σ standard deviation of the final result.

Pressure shift - The transition frequency was measured many times at different pressures in the range of 0.1 - 2 Pa. The results are depicted in Fig. 4, and each data point stands for an averaged value derived from about thirty independent measurements. Both of the linear

fit and the weighted average of the line positions obtained at different pressures are given in Fig. 4(a). Note that the pressure induced shift was reported to be -3.3 kHz/Pa from the Doppler broadened spectra [43], which is considerably larger than the result observed here. Eliminated pressure-induced line shifts in Lamb-dip measurements at low pressures were also observed for different transitions of quite a few molecules [32, 34, 44]. Taking into account the difference between the weighted average and linear fit of the positions obtained at different pressures, we give an uncertainty of 0.5 kHz for the contribution from the pressure dependence of the line center. The collisional or pressure-induced broadening, was also obtained from fitting the spectra and they are plotted in Fig. 4(b). The line width (FWHM) follows a linear dependence on the pressure with a slope of 206(6) kHz/Pa. As a comparison, the self-broadening coefficient was reported to be 77.5(6) kHz/Pa (FWHM) derived from the Doppler broadened spectra recorded between 10 - 600 Torr [45]. The disagreements between low-pressure Lamb-dip measurements and high-pressure Doppler broadened spectra were found for both the pressure broadening and pressure shift coefficients. It has been discussed in our previous work [44], and also was recently investigated by Sears *et al.* [46] indicating rich physics in the collision dynamics of molecules at low pressures.

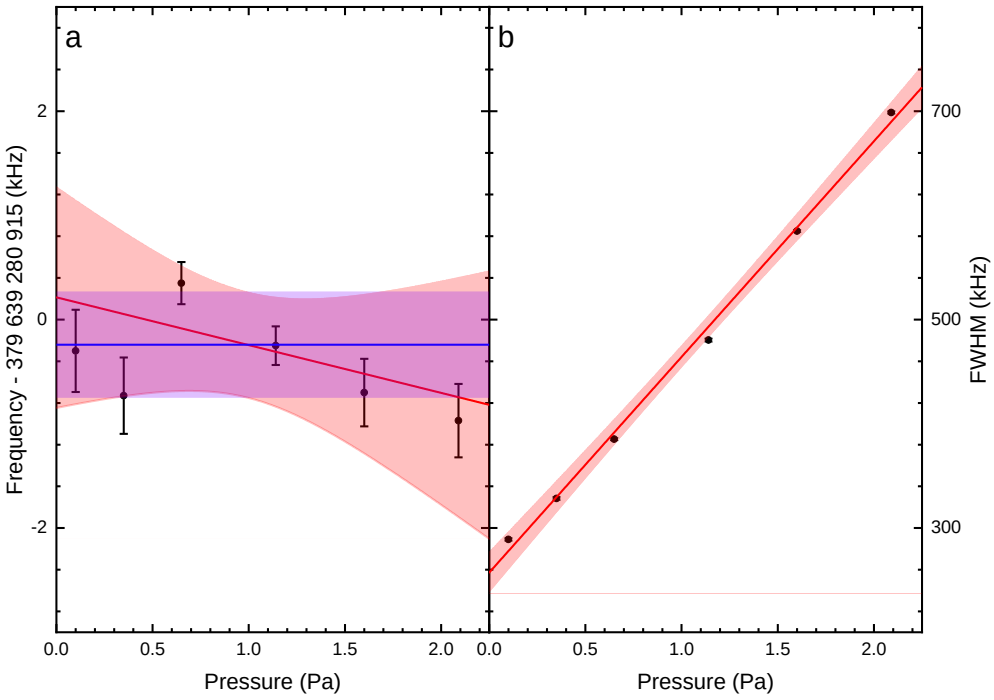

Fig. 4. Line position (a) and line-width (b) of the P(5) line obtained at different sample pressures. The red area was 95% fitting confident interval of the linear fitting. The violet area was 95% fitting confident interval of the 0-slope linear fitting. Both the linear fit and the weighted average of the line positions are shown in panel (a).

Other systematic effects - We have also investigated other experimental parameters which may potentially introduce systematic shifts, such as the laser power and the fiber EOM driving power (modulation index). No detectable shift in the line center was observed, when we reduced half of the laser power or the EOM driving power.

The uncertainty budget of the P(5) line position determined from $1f$ wm-NICE-OHMS measurements is given in Table 1. The statistical uncertainty is 0.2 kHz. Other systematic uncertainties from the effects discussed above are listed in the table. Finally, we determined the line center to be 379 639 280 915.3(1.2) kHz. This value agrees well with our previous result 379 639 280 915.0(3.2) obtained from CRDS measurements.

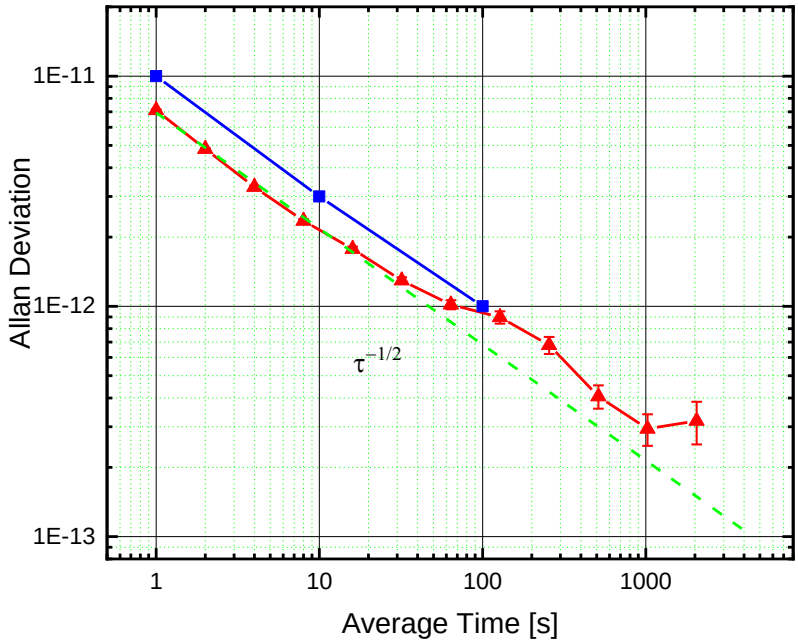

Fig. 5. Allan deviations of the laser locked on the C_2H_2 line using the NICE-OHMS method. Triangles are the beat-note between the NICE-OHMS stabilized laser and a frequency comb. Squares are for the rubidium clock, given by the manufacture.

In order to investigate the long-term stability of the system, we used a feedback servo based on the $2f$ wm-NICE-OHMS signal to control the cavity length through the PZT attached to the HR mirror, which eventually lock the laser to the P(5) line of C_2H_2. Beat frequency between the laser and the frequency comb was recorded and the Allan deviations are shown in Fig. 5. It indicates a stability of $8\times10^{-12}\mathrm{Hz}^{-1/2}$, and reaches about 3×10^{-13} at 1000 s. The fractional frequency uncertainty is primarily limited by the GPS-referenced rubidium clock used in our measurements, and could be potentially improved by replacing it with a hydrogen master. Note that a stability of 10^{-14} has recently been demonstrated by NICE-OHMS [1] without giving an absolute value of the frequency. The work presented here indicates that the NICE-OHMS technique can be potentially used to realize a molecular clock with an accuracy of 10^{-14}, it would be comparative to the best record obtained by J. Ye′s group who used a transition of CH4 in the mid-IR region [16].

4. Conclusion

In summary, we implemented the comb-locked NICE-OHMS technique for frequency metrology study of molecules. It combines extremely high sensitivity and high accuracy as well, being

Optics EXPRESS

Table 1. Uncertainty budget of the position of the P(5) line in the $\nu_1 + 3\nu_3$ band of $^{12}C_2H_2$, in kHz.

Source	Corrections	$\Delta f(1\sigma)$
Statistics	379 639 280 914.7	0.20
Frequency calibration		<0.80
Line profile		<0.30
WM dither Frequency		<0.10
WM dither Amplitude		<0.30
RAM		<0.27
Pressure shift		<0.45
Others		<0.45
Second-order Doppler	+0.60	0
Total	379 639 280 915.3	1.2

a powerful tool to investigate Doppler-free transitions of molecules in the near infrared. The method was demonstrated by studying an overtone transition of C_2H_2 near 789 nm. Compared to the CRDS measurements implemented with the same cavity, the wavelength-modulated NICE-OHMS method improves the signal-to-noise ratio with a factor of 10. Potential sources which may contribute to the systematic shift on the line position were investigated, including the residual amplitude modulation, wavelength modulation amplitude and frequency, and other experimental conditions. An overall uncertainty of 1.2 kHz ($\delta\nu/\nu = 3.2 \times 10^{-12}$) was given to the position of the C_2H_2 line at 12663.40 cm^{-1} determined by NICE-OHMS. We also stabilize a laser to the molecular line using the $2f$ wm-NICE-OHMS signal. A stability of $3{\times}10^{-13}$ was demonstrated for hours, which was mainly limited by the accuracy of our current reference clock.

Funding.

This work was jointly supported by National Key R&D Program of China (2017YFF0206102), the Chinese Academy of Science (XDB21020100), and the National Natural Science Foundation of China (91736101,21688102,91436209,21427804).

References

1. S. Saraf, P. Berceau, A. Stochino, R. Byer, and J. Lipa, "Molecular frequency reference at 1.56μm using a $^{12}C^{16}O$ overtone transition with the noise-immune cavity-enhanced optical heterodyne molecular spectroscopy method," Opt. Lett. **41**, 2189–2192 (2016).
2. T. Oka, "Spectroscopy and astronomy: H_3^+ from the laboratory to the galactic center," Faraday Discuss. **150**, 9 – 22 (2011).
3. C. P. Nicholls, T. Lebzelter, A. Smette, B. Wolff, H. Hartman, H.-U. Käufl, N. Przybilla, S. Ramsay, S. Uttenthaler, G. M. Wahlgren, S. Bagnulo, G. A. J. Hussain, M.-F. Nieva, U. Seemann, and A. Seifahrt", "Crires-pop: a library of high resolution spectra in the near-infrared II. data reduction and the spectrum of the K giant 10 leonis," Astron. & Astrophys. **598**, A79 (2017).
4. M. ReichenbÃđcher and J. Popp, *Challenges in Molecular Structure Determination* (Springer-Verlag Berlin Heidelberg, 2012).
5. Y. Tan, J. Wang, X.-Q. Zhao, A.-W. Liu, and S.-M. Hu, "Cavity ring-down spectroscopy of the fifth overtone of CO," J. Quant. Spectrosc. Radiat. Transf. **187**, 274 – 279 (2017).
6. E. J. Salumbides, G. D. Dickenson, T. I. Ivanov, and W. Ubachs, "QED effects in molecules: Test on rotational quantum states of H_2," Phys. Rev. Lett. **107**, 043005 (2011).

Optics EXPRESS

7. V. I. Korobov, L. Hilico, and J.-P. Karr, "Fundamental transitions and ionization energies of the hydrogen molecular ions with few ppt uncertainty," Phys. Rev. Lett. **118**, 233001 (2017).
8. F. M. J. Cozijn, P. Dupré, E. J. Salumbides, K. S. E. Eikema, and W. Ubachs, "Sub-doppler frequency metrology in HD for tests of fundamental physics," Phys. Rev. Lett. **120**, 153002 (2018).
9. L.-G. Tao, A.-W. Liu, K. Pachucki, J. Komasa, Y. R. Sun, J. Wang, and S.-M. Hu, "Toward a determination of the proton-electron mass ratio from the lamb-dip measurement of HD," Phys. Rev. Lett. **120**, 153001 (2018).
10. C. Chin, V. V. Flambaum, and M. G. Kozlov, "Ultracold molecules: new probes on the variation of fundamental constants," New J. Phys. **11**, 055048 (2009).
11. D. Hanneke, R. A. Carollo, and D. A. Lane, "High sensitivity to variation in the proton-to-electron mass ratio in O_2^+," Phys. Rev. A **94**, 050101 (2016).
12. N. Huntemann, B. Lipphardt, C. Tamm, V. Gerginov, S. Weyers, and E. Peik, "Improved limit on a temporal variation of m_p/m_e from comparisons of Yb^+ and cs atomic clocks," Phys. Rev. Lett. **113**, 210802 (2014).
13. M. S. Safronova, D. Budker, D. DeMille, D. F. J. Kimball, A. Derevianko, and C. W. Clark, "Search for new physics with atoms and molecules," Rev. Mod. Phys. **90**, 025008 (2018).
14. G. Tranter, "Parity-violating energy differences of chiral minerals and the origin of biomolecular homochirality," Nature **318**, 172–173 (1985).
15. M. Quack, J. Stohner, and M. Willeke, "High-resolution spectroscopic studies and theory of parity violation in chiral molecules," Annu. Rev. Phys. Chem. **59**, 741–769 (2008).
16. S. M. Foreman, A. Marian, J. Ye, E. A. Petrukhin, M. A. Gubin, O. D. Mucke, F. N. C. Wong, E. P. Ippen, and F. X. Kartner, "Demonstration of a HeNe/CH_4-based optical molecular clock," Opt. Lett. **30**, 570–572 (2005).
17. M. de Labachelerie, K. Nakagawa, and M. Ohtsu, "Ultranarrow $^{13}C_2H_2$ saturated-absorption lines at 1.5 μm," Opt. Lett. **19**, 840–842 (1994).
18. H. S. Moon, "Frequency stabilization of a 1.3 μm laser diode using double resonance optical pumping in the 5p3/2-6s1/2 transition of Rb atoms," Appl. Opt. **47**, 1097–1102 (2008).
19. K. Nakagawa, T. Katsuda, A. Shelkovnikov, M. de Labachelerie, and M. Ohtsu, "Highly sensitive detection of molecular absorption using a high finesse optical cavity," Opt. Comm. **107**, 369 – 372 (1994).
20. A. Cygan, P. Wcisło, S. Wójtewicz, P. Masłowski, J. Domysławska, R. S. Trawiński, R. Ciuryło, and D. Lisak, "Precise cavity enhanced absorption spectroscopy," J. Phys. Confer. Ser. **548**, 012015 (2014).
21. A. O'Keefe and D. A. G. Deacon, "Cavity ring down optical spectrometer for absorption measurements using pulsed laser sources," Rev. Sci. Instrum. **59**, 2544–2551 (1988).
22. B. A. Paldus and A. A. Kachanov, "An historical overview of cavity-enhanced methods," Can. J. Phys. **83**, 975–999 (2005).
23. S. Kassi and A. Campargue, "Cavity ring down spectroscopy with 5×10^{-13} cm^{-1} sensitivity," J. Chem. Phys. **137**, 234201 (2012).
24. J. Ye, L.-S. Ma, and J. L. Hall, "Ultrasensitive detections in atomic and molecular physics: demonstration in molecular overtone spectroscopy," J. Opt. Soc. Am. B **15**, 6–15 (1998).
25. L.-S. Ma, J. Ye, P. Dubé, and J. L. Hall, "Ultrasensitive frequency-modulation spectroscopy enhanced by a high-finesse optical cavity: theory and application to overtone transitions of C_2H_2 and C_2HD," J. Opt. Soc. Am. B **16**, 2255–2268 (1999).
26. H. Dinesan, E. Fasci, A. D'Addio, A. Castrillo, and L. Gianfrani, "Characterization of the frequency stability of an optical frequency standard at 1.39 μm based upon noise-immune cavity-enhanced optical heterodyne molecular spectroscopy," Opt. Express **23**, 1757–1766 (2015).
27. C. R. Markus, J. N. Hodges, A. J. Perry, G. S. Kocheril, H. S. P. Müller, and B. J. McCall, "High precision rovibrational spectroscopy of OH^+," Astrophys. J. **817**, 138 (2016).
28. A. Foltynowicz, W. Ma, and O. Axner, "Characterization of fiber-laser-based sub-doppler nice-ohms for quantitative trace gas detection," Opt. Express **16**, 14689–14702 (2008).
29. R. Centeno, J. Mandon, S. M. Cristescu, O. Axner, and F. J. M. Harren, "External cavity diode laser-based detection of trace gases with nice-ohms using current modulation," Opt. Express **23**, 6277–6282 (2015).
30. G. Zhao, T. Hausmaninger, W. Ma, and O. Axner, "Shot-noise-limited doppler-broadened noise-immune cavity-enhanced optical heterodyne molecular spectrometry," Opt. Lett. **43**, 715–718 (2018).
31. G. Giusfredi, S. Bartalini, S. Borri, P. Cancio, I. Galli, D. Mazzotti, and P. De Natale, "Saturated-absorption cavity ring-down spectroscopy," Phys. Rev. Lett. **104**, 110801 (2010).
32. J. Wang, Y. R. Sun, L.-G. Tao, A.-W. Liu, and S.-M. Hu, "Communication: Molecular near-infrared transitions determined with sub-khz accuracy," J. Chem. Phys. **147**, 091103 (2017).
33. J. Wang, Y. R. Sun, L.-G. Tao, A.-W. Liu, T.-P. Hua, F. Meng, and S.-M. Hu, "Comb-locked cavity ring-down saturation spectroscopy," Rev. Sci. Instrum. **88**, 043108 (2017).
34. L.-G. Tao, T.-P. Hua, Y. R. Sun, J. Wang, A.-W. Liu, and S.-M. Hu, "Frequency metrology of the acetylene lines near 789nm from lamb-dip measurements," J. Quant. Spectrosc. Radiat. Transf. **210**, 111 – 115 (2018).
35. R. W. P. Drever, J. L. Hall, F. V. Kowalski, J. Hough, G. M. Ford, A. J. Munley, and H. Ward, "Laser phase and frequency stabilization using an optical resonator," Appl. Phys. B **31**, 97–105 (1983).
36. N. C. Wong and J. L. Hall, "Servo control of amplitude modulation in frequency-modulation spectroscopy: demonstration of shot-noise-limited detection," J. Opt. Soc. Am. B **2**, 1527–1533 (1985).
37. R. G. DeVoe and R. G. Brewer, "Laser-frequency division and stabilization," Phys. Rev. A **30**, 2827–2829 (1984).

Optics EXPRESS

38. F. Herregodts, E. Kerrinckx, T. R. Huet, and J. V. Auwera, "Absolute line intensities in the $\nu_1 + 3\nu_3$ band of $^{12}C_2H_2$ by laser photoacoustic spectroscopy and fourier transform spectroscopy," Mol. Phys. **101**, 3427–3438 (2003).
39. P. Kluczynski, J. Gustafsson, Å. M. Lindberg, and O. Axner, "Wavelength modulation absorption spectrometry-an extensive scrutiny of the generation of signals," Spectrochim. Acta Part B **56**, 1277 – 1354 (2001).
40. T.-L. Chen and Y.-W. Liu, "Sub-doppler resolution near-infrared spectroscopy at 1.28μm with the noise-immune cavity-enhanced optical heterodyne molecular spectroscopy method," Opt. Lett. **42**, 2447–2450 (2017).
41. M. Gehrtz, G. C. Bjorklund, and E. A. Whittaker, "Quantum-limited laser frequency-modulation spectroscopy," J. Opt. Soc. Am. B **2**, 1510–1526 (1985).
42. L. Li, F. Liu, C. Wang, and L. Chen, "Measurement and control of residual amplitude modulation in optical phase modulation," Rev. Sci. Instrum. **83**, 043111 (2012).
43. F. Herregodts, M. Hepp, D. Hurtmans, J. Vander Auwera, and M. Herman, "Laser spectroscopy of the $\nu_1 + 3\nu_3$ absorption band in $^{12}C_2H_2$. ii. self-collisional lineshift measurements," J. Chem. Phys. **111**, 7961–7965 (1999).
44. J. Chen, T.-P. Hua, L.-G. Tao, Y. Sun, A.-W. Liu, and S.-M. Hu, "Absolute frequencies of water lines near 790 nm with 10^{-11} accuracy," J. Quant. Spectrosc. Radiat. Transf. **205**, 91 – 95 (2018).
45. F. Herregodts, D. Hurtmans, J. Vander Auwera, and M. Herman, "Laser spectroscopy of the $\nu_1 + 3\nu_3$ absorption band in $^{12}C_2H_2$. i. pressure broadening and absolute line intensity measurements," J. Chem. Phys. **111**, 7954–7960 (1999).
46. S. Twagirayezu, G. E. Hall, and T. J. Sears, "Frequency measurements and self-broadening of sub-doppler transitions in the $\nu_1 + \nu_3$ band of $^{12}C_2H_2$," J. Chem. Phys. **149**, 154308 (2018).